STRUCTURAL CAPACITIES OF H-SHAPED RC CORE WALL SUBJECTED TO LATERAL LOAD AND TORSION

Makoto MARUTA[1], Norio SUZUKI[2], Takashi MIYASHITA[3] And Takamasa NISHIOKA[4]

SUMMARY

This paper describes an experimental and analytical study on H-shaped RC core walls subjected to simultaneous lateral load and torsion. The torsional stiffness of an open section core wall (OSCW) is smaller than that of a closed section one (CSCW). It is predicted that the elasto-plastic capacities of OSCW are inferior to those of CSCW. However, few researches have been carried out on the elasto-plastic torsional behavior of OSCW. When a high-rise RC structure with OSCW is designed in an aseismic country, it is important to evaluate the structural capacities of OSCW, especially H-shaped core wall subjected to simultaneous lateral load and torsion. The correlation between the maximum lateral strength and the maximum torsional strength is especially important. Nine H-shaped core walls were tested under simultaneous lateral load and torsion. Two parameters were studied: the ratio of torsion to lateral load and the lateral load direction of the H-shaped wall. All specimens were designed to reach flexural yielding before shear failure. Nonlinear finite element analyses were carried out to verify the test results, and to obtain the data of untested cases.

The following results are obtained: (1) the maximum lateral strength decreases with increase in torsion. (2) the bending-torsional resistant mechanism of an H-shaped wall varies depending on the loading direction. (3) the correlation curves at maximum strengths were close to elliptical for each direction, making the overall correlation spherical.

INTRODUCTION

Recently, several high-rise RC structures with core walls have been designed and constructed in Japan. Due to architectural planning requirements, these core walls have often been of the open section type, typically H-shaped. They would be subjected to simultaneous lateral load and torsion in an earthquake. The lowest portion of the core walls is subjected to especially large bending moment and torsion.

The design procedure for a column or a closed section wall subjected to lateral load and torsion is prescribed in the ACI code [ACI, 1995], etc. The ACI code describes the limit of torsional moment, and the reinforcing method required when the torsional moment exceed this limit.

However, there are unknown factors concerning the structural capacities of an open section core wall (OSCW) subjected to simultaneous lateral load and torsion. Each plate of a closed section core wall (CSCW) like a box-section subjected to pure torsion is likely in the pure shearing state. Because of the warping of OSCW, its flange walls are subjected to bending moment and shear, so the ACI design method for torsion can not be applied to OSCW. Therefore, experimental and analytical studies were carried out to determine the elaso-plastic behavior of OSCW, especially H-shaped core walls.

[1] *Kajima Technical Research Institute, Kajima Corp., Japan Email: maruta@katri.kajima.co.jp*
[2] *Kajima Technical Research Institute, Kajima Corp., Japan Email: nsz@katri.kajima.co.jp*
[3] *Information Processing Center, Kajima Corp., Japan E-mail: miyashita@ipc.kajima.co.jp*
[4] *Nuclear Power Department, Construction Group, Kajima Corporation E-mail: nisioka@psa.kajima.co.jp*

This paper describes the test results and analytical results, and the correlation between maximum bending and the maximum torsional moment derived from these results. The correlation between bending and torsion is important for design of a high-rise structure's core wall, because the lowest portion of the wall is in the most severe condition under earthquake load. In particular, the bending moment is more severe than the shear force.

STRUCTURAL TEST

Specimens and Test Method

Nine 1/12 scale specimens as listed in Table 1 were tested. All specimens had the same H-shaped section, were the same size and had the same reinforcement. Fig.1 shows the details of the specimens. They had column type reinforcement at both flange edges. Experimental parameters were the lateral loading direction and the ratio of torsional moment to bending moment at the lowest portion of the wall. The loading directions were the strong axis for Series 1, the weak axis for Series 2 and the diagonal axis for Series 3, as shown in Fig.2.

The ratios of torsional moment (*T*) to bending moment (*M*) at the lowest portion of the wall were varied: 0%, 25%, 50%, 75% and 100%. These ratios are called the torsional ratio. The torsional ratio was the main parameter of this test.

The material properties are shown in Table 2. The maximum size of concrete coarse aggregate was 10mm diameter, and the target compressive strength was 60N/mm^2 at the time of test.

The torsion is born mainly by the flange walls. Therefore, the elastic moment distributions of the flange walls are predicted as shown in Fig.2. The torsional capacities of Series 1 were assumed to be influenced by the magnitude of the axial stress in each flange. If the lateral force became bigger, the axial stresses between flange 1 and flange 2 varied more. Its stress has a large influence on torsion resisted by each flange in the in-plane direction.

In Series 2, only the flange walls resist the bending moment and torsion. The moment distributions of the flanges are assumed to vary with the torsional ratio, as shown in Fig.2. The behavior of Series 3 may be between those of Series 1 and Series 2.

The tests were conducted using the six-degree-of freedom apparatus shown in Photo 1. This apparatus can impose a torsional moment that is proportional to the constant ratio of bending moment at the lowest portion of the walls.

The weight of a loading plate and the loading slab, 118 kN, was applied as the axial force to the specimen. A cyclic loading was applied at

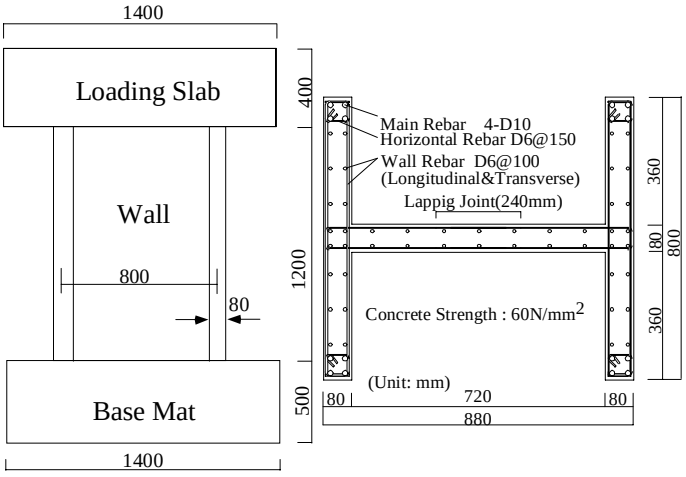

Fig. 1: Test Specimens

Table 1: List of Test Specimen

Series	Specimen	Loading Direction	Loading Ratio(%) (M : T*1.)
1	HS25	Strong	75 : 25
	HS50		50 : 50
	HS75		25 : 75
2	HW00	Weak	100 : 0
	HW25		75 : 25
	HW50		50 : 50
	HW75		25 : 75
3	HD25	Diagonal	75 : 25
4	H100	Pure Torsion	0 : 100

M: Bending Moment at Lowest Portion T: Torsional Moment
*1 : Torsional Ratio

Table 2: Material Properties

(Concrete)

Specimen	Sealed in Field		
	Compressive Strength (N/mm^2)	Young's Modulus (*10^4 N/mm^2)	Tensil Strength (N/mm^2)
HS25	57.6	3.02	3.05
HS50	59.3	2.98	3.29
HS75	60.4	2.83	3.48
HW00	56.1	3.58	2.79
HW25	57.9	3.46	3.74
HW50	57.8	2.89	3.12
HW75	64.1	3.25	2.94
HD25	62.5	3.13	3.47
H100	66.4	3.10	4.00

(Rebar)

Diameter	Yeild Point ₱y (N/mm^2)	Tensile Strength ₱t (N/mm^2)	Yieilding Strain Å y@i*10^{-6}j	Elongation (%)
D6	365	419	1972	17.9
D10	403	595	2145	25.3

each target drift angle (R1) that was defined in Fig.3, of 1/800, 1/400, 1/200, 1/100, 1/50, 1/25. δ_R is the average lateral displacement in the loading direction, and δ_θ is the rotational displacement, as shown in Fig.3.

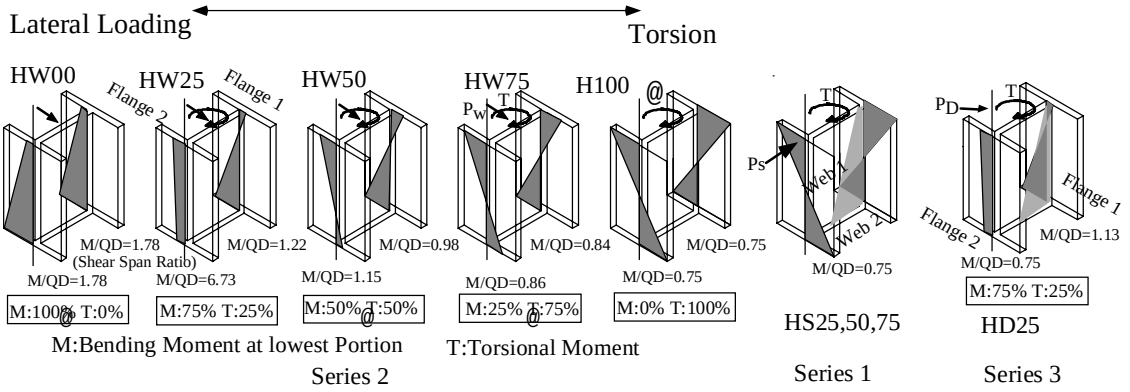

Fig.2: Assumed Moment Distribution of Specimen

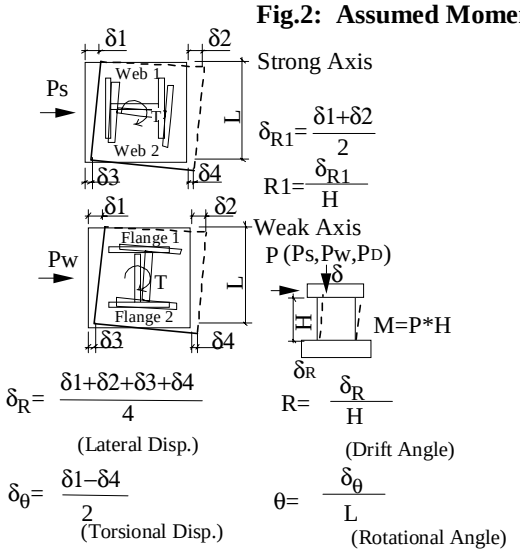

Fig. 3: Measurement and Evaluation of Displacement

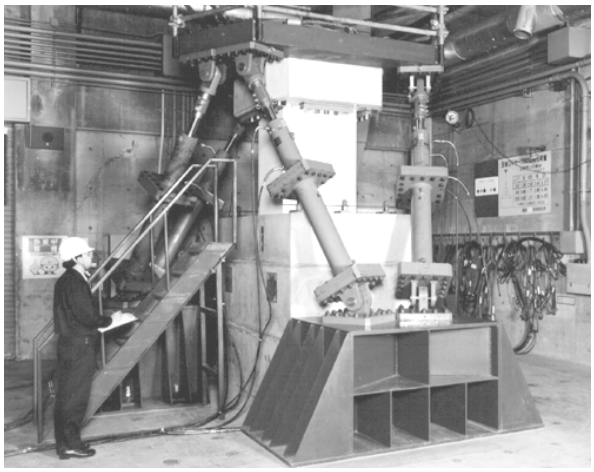

Photo 1: Test Setup

Table 3: Test Results

Specimen	Elastic stiffness	Bending Crack (Flange)		Shear Crack (Flange)		Yeilding of Column Rebar		Yeilding of Transverse Rebar of Wall		Maximum Strength	
	K_δ *1	M*3	R*5	M	R	M	R	M	R	M	R
	K_θ *2	T*4	δ_θ *6	T	δ_θ	T	δ_θ	T	δ_θ	T	δ_θ
HS25	4973	71	0.04	—	—	271	2.25	425	13.6	468	32.7
	103200	6	0.04	—	—	89	3.51	124	20	153	46.5
HS50	4916	79	0.28	106	0.53	139	1.36	190	2.31	235	7.46
	88400	69	1.61	100	2.43	131	4.99	177	8.16	228	22.2
HS75	4690	38	0.16	50	0.46	60	0.67	79	1.59	93	6.34
	7900	12	2.24	143	4.78	167	6.81	227	13	283	32.8
HW00	1990	100	0.90	243	4.61	145	2	450	19.1	459	23.8
	—	—	—	—	—	—	—	—	—	—	—
HW25	2120	95	0.39	315	3.35	250	1.97	423	15.1	426	12.7
	64100	32	0.59	101	4.65	82	2.57	135	21.3	137	18.6
HW50	2030	57	0.29	122	0.91	122	0.91	172	2.1	214	5.06
	91500	57	0.39	117	2.89	117	2.89	162	6.63	205	16
HW75	1630	20	0.12	51	0.82	61	0.84	97	1.17	87	3.29
	74800	54	0.96	148	4.85	168	6.93	197	9.26	251	18.9
HD25 Positive	3591	133	0.42	240	1.3	341	2.9	487	9.9	529	12.5
	65200	43	0.73	76	1.79	109	4.3	161	15.1	171	18.5
Negative		-79	-0.09	-192	-0.98	-223	-1.33	—	—	-390	-10.9
		-22	-0.14	-61	-2.07	-69	-2.8	—	—	-120	-23.1
H100	—	—	—	—	—	—	—	—	—	—	—
	11600	88	1.65	205	9.24	216	10.3	216	10.3	268	22.1

*1: Elastic Stiffness of Lateral Load (kN/cm) *2: Elastic Stiffness of Torsion (kNm/rad)

*3: Bending Moment at Lowest Portion(kNm) *4: Torsional Moment(kNm) *5: Drift Angle($*10^{-3}$rad)

*6: Rotational Angle($*10^{-3}$rad)

TEST RESULTS

The test results are listed in Table 3. All specimens reached flexural yielding before shear failure.
The load and deflection curves (M -δ_R , T-δ_θ) of HS25, HW25, HW75 and HD25, are shown in Fig.4 for examples.
For Series 1 (HS25), the both load-deflection curves of M -δ_R and T-δ_θ showed pinching behavior after shear cracking. No decline in maximum strength was observed after the flange yielded, because of the small torsion ratio. It showed a good energy absorbing hystereris loop. One of flanges that was under compression due to the lateral load didn't yield until the large displacement region.
At Series 2, HW25 showed a good hystereris loop before R=1/100. The damage to the flange was more severe than that of the HS25's. Both flanges of HW25 had yielded by R=1/50.
As the torsional effect of HW75 was bigger than that of HW25, HW75 had many shear cracks in both flanges. The pinching behavior of HW75 after shear cracking was more remarkable than that of HW25.
At Series 3, the axial force of flanges fluctuated between positive and negative loading, as shown in Fig.5. In this figure, the F2B portion was in a full compressive state under positive loading, and in a full tensile state under negative loading. Therefore, the load-deflection curves of HD25 showed different behavior under positive

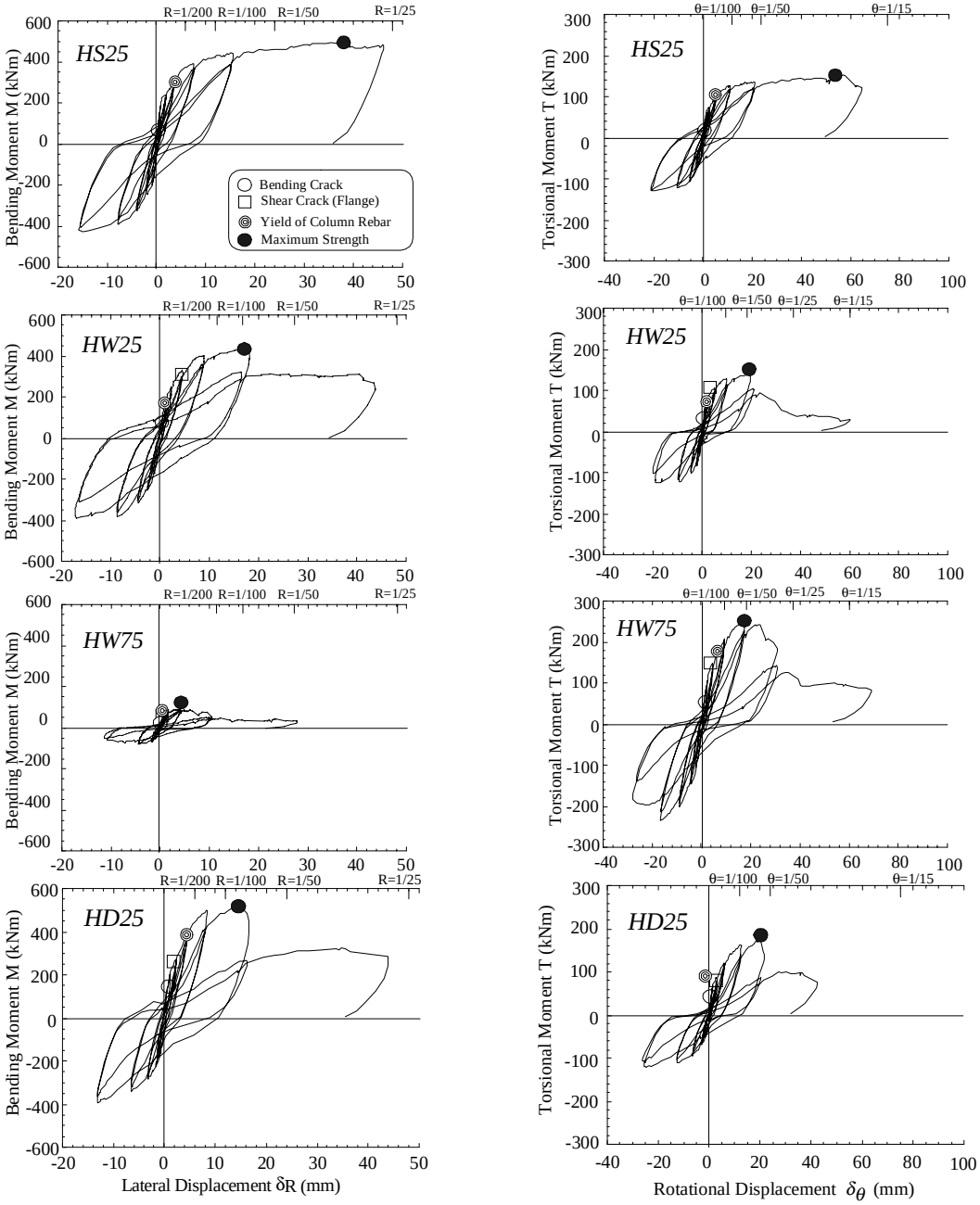

Fig. 4: Load-Deflection Curves

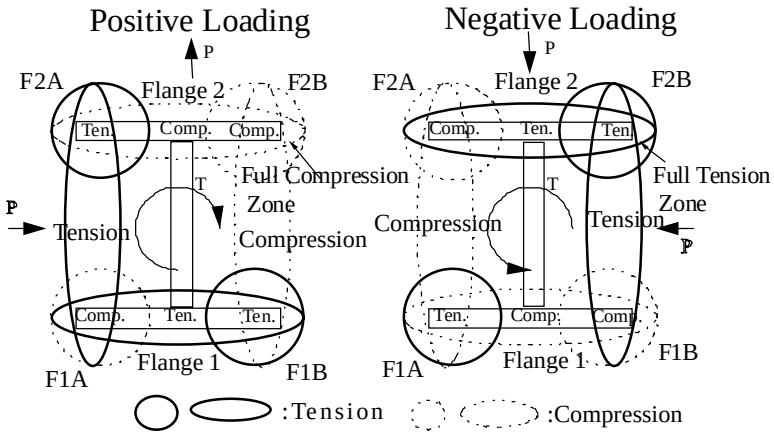

*:Diagonal Force is distributed to strong and weak forces

Fig. 5: Axial Force Distribution of Series 3

and negative loading.

The comparison of specimens with the torsional moment ratio of 25•, shows that the specimen subjected to strong axis lateral loading (HS25) had better ductility than the specimens subjected to weak axis and the diagonal axis loading.

FINITE ELEMENT ANALYSIS (FEM)

A nonlinear finite element analysis was conducted to verify the test results and, to obtain the data of untested cases.

Analytical Model

The concrete and rebars were modeled as a layered shell element [Miyashita et all, 1991] as shown in Fig. 6. In this analysis, the stress and strain of the concrete was calculated for each layer. The rebars were idealized as a layered plate element that had the equivalent stiffness in the rebar direction. The stress-strain relationship of the rebars was modeled by as bi-linear. The stress-strain relationship of the concrete was modeled as shown in Fig. 7. Model details are as follows;

1) The stress-strain relationship is evaluated on each principal axis assuming orthogonal anisotropy.
2) The deteriorate ratio β of compressive strength is defined as in Eq. 1.

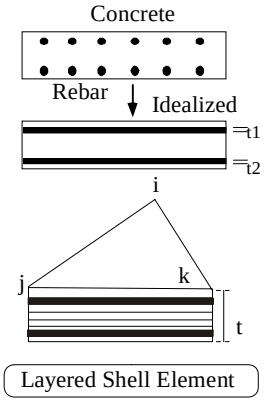

Fig. 6: Finite Element Model

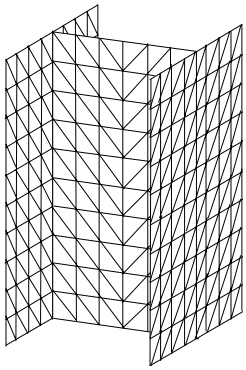

Fig. 8: Mesh Layout

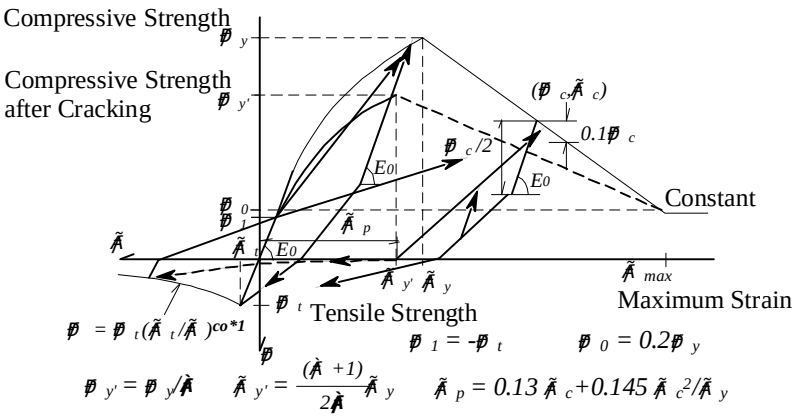

$\sigma_{y'} = \sigma_y/\alpha$ $\varepsilon_{y'} = \frac{(\alpha+1)}{2\alpha}\varepsilon_y$ $\varepsilon_p = 0.13\varepsilon_c + 0.145\varepsilon_c^2/\varepsilon_y$

$\sigma = \sigma_t(\varepsilon_t/\varepsilon)^{co*1}$ $\sigma_1 = -\sigma_t$ $\sigma_0 = 0.2\sigma_y$

Fig.7: Analytical Model of Concrete

$$\beta = 0.8 + 0.6\left\{(\varepsilon_1 + 0.0002)\times 10^3\right\}^{0.39} \quad \cdots\cdots\cdots \text{ (Eq. 1)}$$

ε_1 : Orthogonal strain to crack direction

3) The shear stiffness *G* after cracking is based on Aoyagi's proposal [Aoyagi et all, 1981] as shown in Eq. 2.

$$G = 1/\left(\frac{1}{Ge} + \frac{1}{3.6/\varepsilon_1}\right) \quad \left(N/mm^2\right) \quad \cdots\cdots\cdots \text{ (Eq. 2)}$$

Ge : Elastic shear modulus

4) The tensile response of cracked concrete*[1] is shown in Fig. 7. The multiplier *CO* in Fig. 7 is a coefficient depending on bond characteristics. The tension stiffness of an element is determined by *CO*. The value of *CO* is 2. 0 for a bending-cracked portion and 0. 4 [Okamura et all, 1987] for a shear-cracked portion. Because *CO*=0. 4 was proposed for shear, it can't accurately express the bond behavior and the rebar stress in the bending cracked portion. *CO*=2. 0 is used to suppress the effect of tension stiffness.

Fig. 8 shows the mesh layout for the specimen.

Analytical Results

Fig. 9 compares the load-deflection curves obtained from the tests and analyses on specimens HS25, HW25 and HD25. The analysis was stopped at the first unstable step under a downgrade. The analytical results follow the experimental results well until the maximum strength, but doesn't represent the pinching behavior well in the large displacement region. The remaining analytical results not shown in Fig. 9 follow the test results for each specimen well. However, the analyzed stiffness is slightly higher than the experimental stiffness in the small loading region.

CORRELATION OF MAXIMUM LOADS

The untested cases were analyzed by the same FEM method. Four cases were analyzed: HS00 (strong axis),

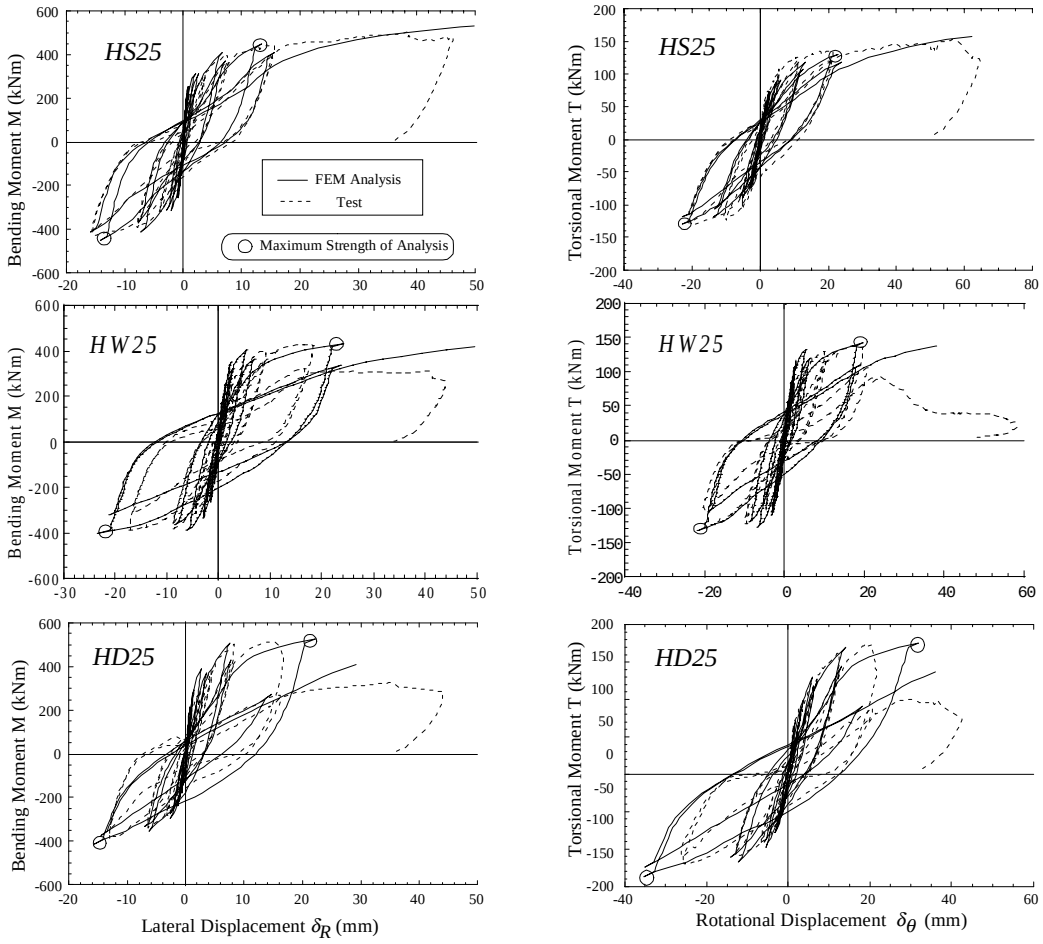

Fig.9: Load-Deflection Curves (Comparisons of Tests and Analyses)

HD00 (diagonal axis), HD50 (diagonal axis) and HD75 (diagonal axis).
The relationships between the maximum torsional moments and the maximum bending moments are plotted in Fig. 10, Fig. 11 and Fig. 12 for each loading direction. These figures include the test results and the analytical results. It is understood from these figures that the bending strength doesn't deteriorate significantly until 25%

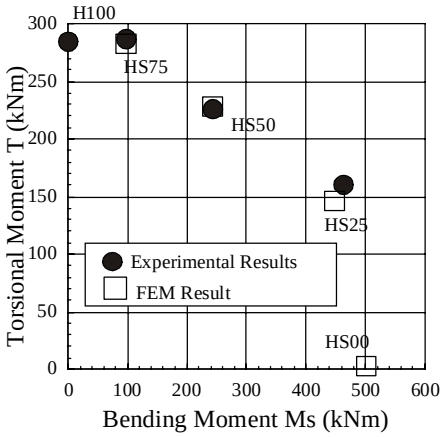

Fig. 10: Correlation between T and Ms (Strong Axis Loading) Series 1

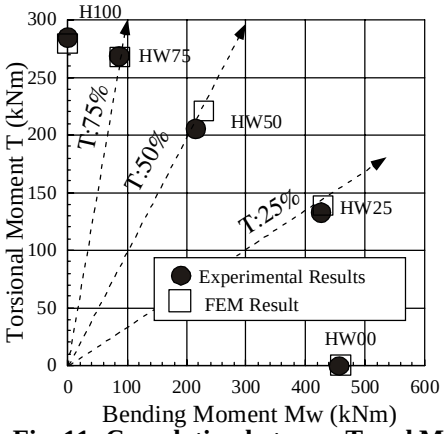

Fig. 11: Correlation between T and Mw (Weak Axis Loading) Series 2

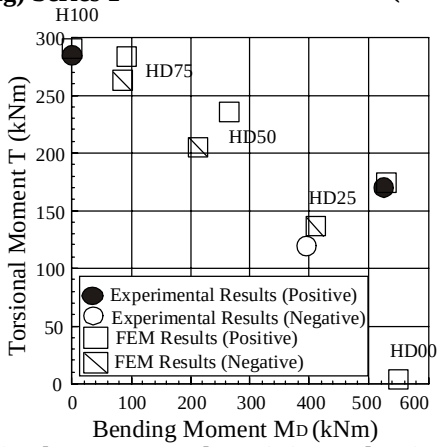

Fig. 12: Correlation between T and M_D (Diagonal Axis Loading) Series 3

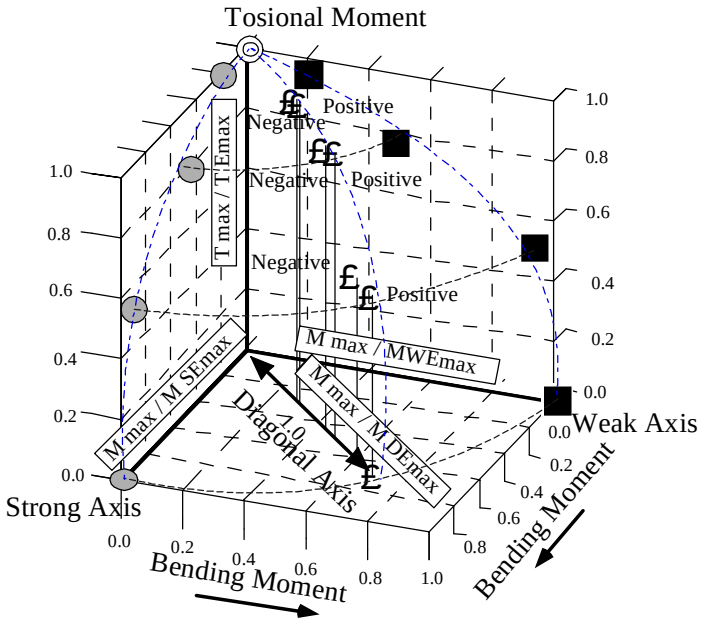

Fig.13: Correlation between Torsional Moment and Bending Moment

of the torsional ratio.
For series 3, the load-deflection curves for positive and negative loading are different, as shown in Fig.4. This is caused by the difference in the flange's axial stress, as shown in Fig. 5. The maximum values for positive and negative loading are also different. They become close as the torsional ratio becomes large, as shown in Fig.12. This is because the fluctuation of axial stress, as shown in Fig.5, become smaller when the torsional ratio become larger.
Fig. 13 shows the relationship between the normalized bending moments in each direction and the normalized torsional moment. The maximum bending moments (M max) in each direction obtained from the tests and the analyses, are normalized by the maximum bending moments in each loading direction (M SEmax, M WEmax and M DEmax) of the non-torsional specimens. The torsional moments are normalized by the non-bending specimen's maximum moment (TE max).
The correlation between bending and torsion of the H-shaped core wall is likely to be spherical, i.e., similar to the M-N interaction curves of a column.
From this relationship, it is possible to design an H-shaped core wall subject to simultaneous lateral load and torsion. In practical design of an H-shaped core wall, the bending moment and pure torsional moment strengths are calculated under the assumption of external force distribution. Next, the flexural capacities are reduced according to the spherical correlation, as shown in Fig. 13.

CONCLUSIONS

Through tests and analyses of H-shaped RC core walls, the following conclusions were reached:
(1) The resistant mechanism of an H-shaped wall subjected to simultaneous bending and torsion varies depending on the loading direction. The web can't resist torsion. Torsinal capacities are influenced by the torsional moment ratio. Torsional capacities under a strong axial loading deteriorate with increasing flange axial stresses. Those under a weak axis loading depend on the changing moment distribution of the flanges.
(2) The bending strength scarcely deteriorate while the torsional moment is under 25%.
(3) The nonlinear finite element method can adequately simulate the hysteric behavior of the test specimens. The maximum bending moment and torsional moment obtained from these analyses correspond closely with the test results.
(4) The correlation of lateral load and torsion was determined for each loading direction. The correlation curves at maximum strengths are very nearly elliptical for each direction. The overall correlation is close to spherical.

REFERENCES

American Concrete Institute 318 (1995), "Building Code Requirements for Reinforced Concrete"
Hayami, Y. , Miyashita, T. and Maeda, T. (1991), "Nonlinear analysis of shear walls", *4th International Conference on Nonlinear Engineering Computations, September*.
Aoyagi, Y. , Ohmori, S. and Yamada, K. (1981), "Strength and deformation characteristics of orthogonally reinforced concrete containments models subjected to lateral forces", *6th SMIRT Conference, J4/5,Paris, France*.
Okamura, H. , Maekawa, K. and Izumo, J. (1987), "Reinforced Concrete Plate Element Subjected to Cyclic Loading", *IABSE Colloquium, Delft, pp575~pp590.*